

# Hyperbolic Pascal pyramid

László Németh\*

## Abstract

In this paper we introduce a new type of Pascal's pyramids. The new object is called hyperbolic Pascal pyramid since the mathematical background goes back to the regular cube mosaic (cubic honeycomb) in the hyperbolic space. The definition of the hyperbolic Pascal pyramid is a natural generalization of the definition of hyperbolic Pascal triangle ([2]) and Pascal's arithmetic pyramid. We describe the growing of hyperbolic Pascal pyramid considering the numbers and the values of the elements. Further figures illustrate the stepping from a level to the next one.

*Key Words:* Pascal pyramid, cubic honeycomb, regular cube mosaic in hyperbolic space.  
*MSC code:* 52C22, 05B45, 11B99.

## 1 Introduction

There are several approaches to generalize the Pascal's arithmetic triangle (see, for instance [3]). A new type of variations of it is based on the hyperbolic regular mosaics denoted by Schläfli's symbol  $\{p, q\}$ , where  $(p-2)(q-2) > 4$  ([5]). Each regular mosaic induces a so called hyperbolic Pascal triangle (see [2, 7]), following and generalizing the connection between the classical Pascal's triangle and the Euclidean regular square mosaic  $\{4, 4\}$ . For more details see [2], but here we also collect some necessary information.

The hyperbolic Pascal triangle based on the mosaic  $\{p, q\}$  can be figured as a digraph, where the vertices and the edges are the vertices and the edges of a well defined part of lattice  $\{p, q\}$ , respectively, and the vertices possess a value that give the number of different shortest paths from the base vertex to the given vertex. Figure 1 illustrates the hyperbolic Pascal triangle when  $\{p, q\} = \{4, 5\}$ . Here the base vertex has two edges, the leftmost and the rightmost vertices have three, the others have five edges. The quadrilateral shape cells surrounded by the appropriate edges correspond to the squares in the mosaic. Apart from the winger elements, certain vertices (called "Type A") have 2 ascendants and 3 descendants, while the others ("Type B") have 1 ascendant and 4 descendants. In the figures we denote vertices type A by red circles and vertices type B by cyan diamonds, further the wingers by white diamonds (according to the denotations in [2]). The vertices which are  $n$ -edge-long far from the base vertex are in row  $n$ . The general method of preparing the graph is the following: we go along the vertices of the  $j^{\text{th}}$  row, according to the type of the elements (winger, A,

---

\*University of West Hungary, Institute of Mathematics, Hungary. [nemeth.laszlo@emk.nyime.hu](mailto:nemeth.laszlo@emk.nyime.hu)



vertices to a certain vertex  $V$  form an icosahedron in this mosaic. It means, considering an arbitrary vertex  $V$  of the mosaic, that the number of cubes around  $V$  is as many as the number of the faces of the icosahedron, namely 20 and the number of the mosaic edges from  $V$  (degree of  $V$ ) is as many as the number of vertices on an icosahedron, namely 12. There are 5 cubes around a mosaic edge as there are 5 faces around a vertex on the icosahedron. In Figure 2 we can see a vertex figure with one cube and the twenty cubes around the centre  $V$  of the icosahedron. Vertex  $X$  and  $W$  are two nearest vertices of the mosaic to  $V$  and around the edge  $V$ - $W$  there are 5 cubes. We mention that the edges of the icosahedron are not the edges of the mosaic, they are the face diagonals of the cubes.

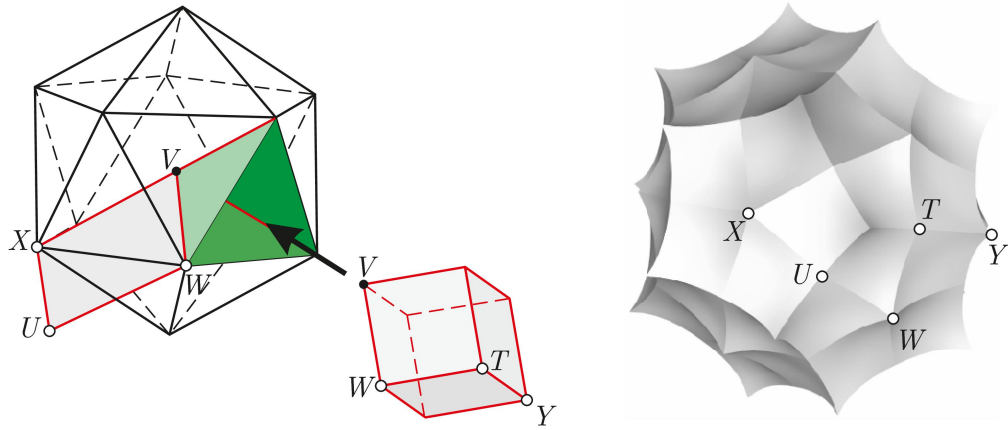


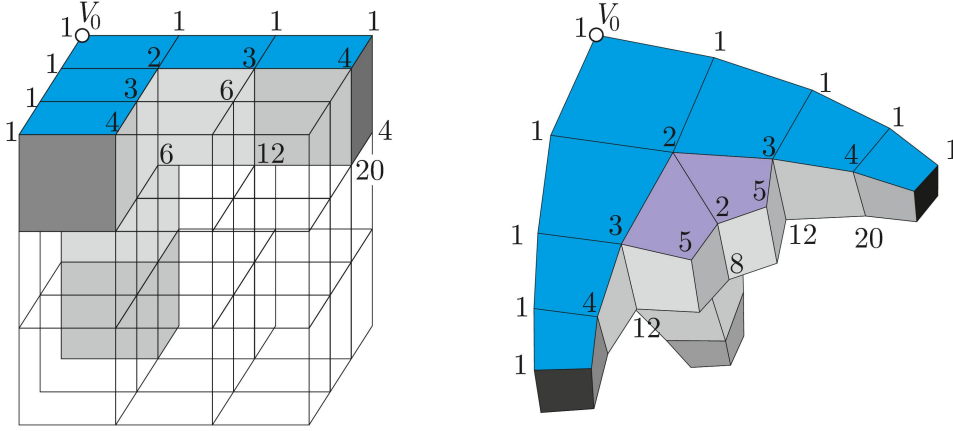
Figure 2: Vertex figure of  $V$  and cubes around  $V$

Now, we consider the hyperbolic (and Euclidean) cubic honeycomb. We define the part  $\mathcal{P}$  of the mosaic which can induce the hyperbolic Pascal pyramid (and the classical Pascal's pyramid).

Take a cube of the mosaic as a base cell of  $\mathcal{P}$  and let  $V_0$  be a vertex of it. Take the three cubes of the mosaic which have common faces with the base cell but do not contain  $V_0$ . (In the right part of Figure 3 we can see the construction of  $\mathcal{P}$  and by comparison the left part shows the Euclidean one.) Reflect these cubes across their own faces which are opposite the touching faces with the base cube. Reflect again the new cubes across the faces which are opposite the previous cubes, and so on limitless. This way we give the "edge"s of the border of  $\mathcal{P}$  (blue cubes in Figure 3) and the convex parts of the mosaic-levels defined by any two "edge"s give the border of  $\mathcal{P}$ . Finally, the convex part of the bordered parts of the mosaic is the well defined  $\mathcal{P}$ . The shape of this convex part of the mosaic resembles an infinite tetrahedron.

Let  $\mathcal{G}_{\mathcal{P}}$  be the graph, in which the vertices and edges are the vertices and edges of  $\mathcal{P}$ . We label an arbitrary vertex  $V$  of  $\mathcal{G}_{\mathcal{P}}$  by the number of different shortest paths along the edges of  $\mathcal{P}$  from  $V_0$  to  $V$ . We mention that all the edges of the mosaic are equivalent. Some labelled vertices can be seen in Figure 3. Let the labelled  $\mathcal{G}_{\mathcal{P}}$  be the hyperbolic Pascal pyramid (more precisely the hyperbolic Pascal tetrahedron), denoted by  $\mathcal{HPP}$ . Considering the Euclidean mosaic  $\{4, 3, 4\}$  instead of the hyperbolic one in the definition above the classical Pascal's pyramid returns.

Let level 0 be the vertex  $V_0$ . Level  $n$  consists of the vertices of  $\mathcal{HPP}$  whose edge-distances

Figure 3: Construction of the border of  $\mathcal{P}$ 

from  $V_0$  are  $n$ -edge (the distance of the shortest path along the edges of  $\mathcal{P}$  is  $n$ ). It is clear, that the labelled graphs indicated by the outer boundaries of  $\mathcal{P}$  are the hyperbolic Pascal triangles based on the regular hyperbolic planar mosaic  $\{4, 5\}$ .

The right part of Figure 4 shows the hyperbolic Pascal pyramid up to level 4, when the digraph  $\mathcal{G}_{\mathcal{P}}$  is directed from  $V_0$  according to the growing distance from  $V_0$  (compare Figures 3 and 4). Moreover, Figures 5 and 6 show the growing from a level to the next one in case of some lower levels. The colours and shapes of different types of the vertices are different. (See the definitions later.) The numbers without colouring and shapes refer to vertices in the lower level in every figure. The graphs growing from a level to the new one contain graph-cycle with six nodes. These graph-cycles figure the convex hulls of the parallel projections of the cubes from the mosaic, where the direction of the projection is not parallel to any edges of the cubes.

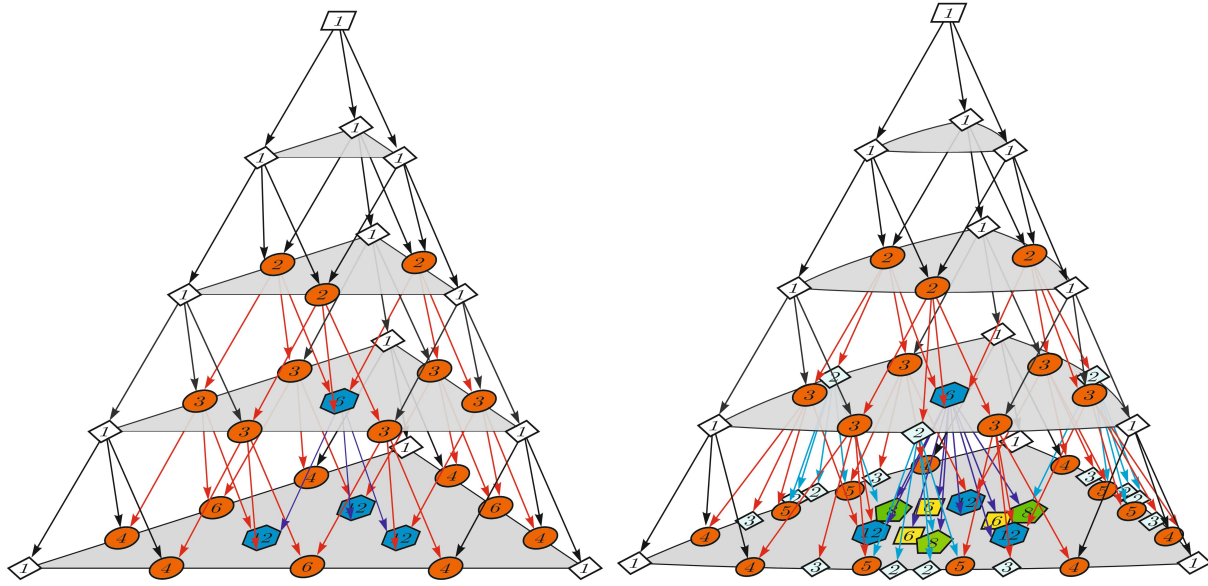
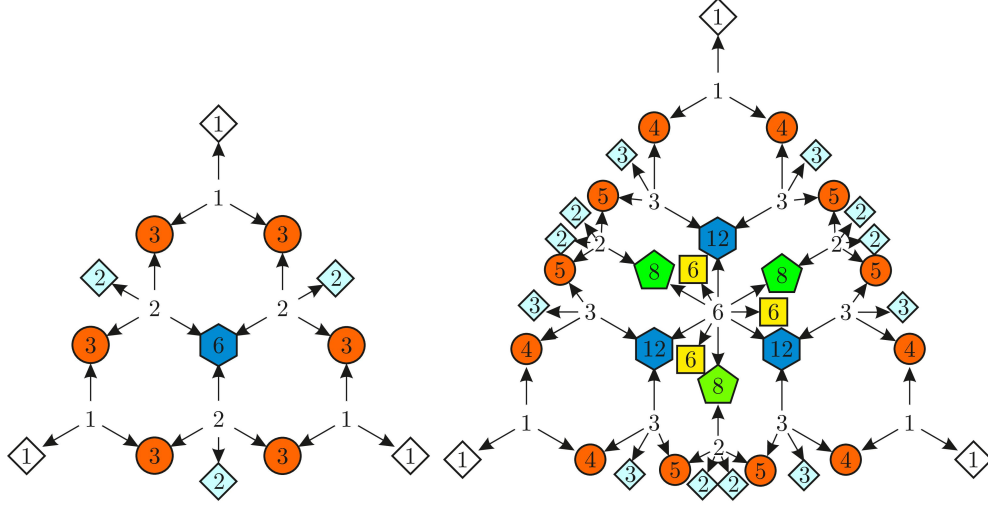


Figure 4: Euclidean and hyperbolic Pascal pyramid

Figure 5: Connection between levels two, three and four in  $\mathcal{HPP}$ 

In the following we describe the method of the growing of the hyperbolic Pascal pyramid and we give the sum of the paths connecting vertex  $V_0$  and level  $n$ .

### 3 Growing of the hyperbolic Pascal pyramid

In the classical Pascal's pyramid the number of the elements on level  $n$  is  $(n+1)(n+2)/2$  and its growing from level  $n$  to  $n+1$  is  $n+2$ , on the contrary in the hyperbolic Pascal pyramid it is more complex.

As the faces of  $\mathcal{HPP}$  are the hyperbolic Pascal triangles, then here are three types of vertices  $A$ ,  $B$  and  $1$  corresponding to the Introduction and [2]. From all  $A$  and  $B$  start only one edge to the inside of the pyramid, because five cubes close around an edge of the mosaic (see Figure 3). The types of inside vertices of these edges differ from the types  $A$  and  $B$ , denote them by type  $C$  and type  $D$ , respectively. The left part of Figure 7 presents a cube, in which the upper face is on the border of  $\mathcal{HPP}$  and a vertex  $A$  on level  $i$  generates a vertex  $C$  inside of  $\mathcal{HPP}$  with 3 incoming edges. The right part shows that all vertices  $B$  imply a vertex  $D$  with two incoming edges.

The growing methods of them are illustrated in Figure 8 (compare it with the growing method in [2]).

As a cube has three edges in all vertices, then during the growing (step from level  $i-1$  to level  $i$ ) an inner arbitrary vertex  $V$  on level  $i$  can be reached from level  $i-1$  with three, two or just one edges. This fact allows us a classification of the inner vertices. Let the type of a vertex on level  $i$  is  $C$ ,  $D$  or  $E$ , respectively, if it has three, two or one joining edges to level  $i-1$  (as before). Figure 9 shows vertex figures of the inner vertices of  $\mathcal{HPP}$ . Vertices  $W_{i-1}$  (small green circles) are on level  $i-1$ , we don't know their types (or not important to know) and the centres are on level  $i$ . The other vertices of the icosahedron are on level  $i+1$  and the classification of them gives their types. An edge of the icosahedron and its centre  $V$  determine a square (a face of a cube) from the mosaic. (Recall, that an edge of the icosahedron is a diagonal of a face of a cube from the mosaic.) Since from a vertex of



a square we can go to the opposite vertex two ways, then a vertex  $X$  of the icosahedron, where  $X$  and a  $W_{i-1}$  are connected by an edge, can be reached with two paths from level  $i - 1$ . (For example in Figure 2, between vertex  $W$  and  $X$  there are the paths  $W - V - X$  and  $W - U - X$ .) So, the type of the third vertex of the faces on the icosahedron whose other two vertices are  $W_{i-1}$  are  $C$ . The types of the vertices which connect to only one  $W_{i-1}$  with icosahedron-edge are  $D$ , the others are type  $C$ . See Figure 9. In case of the vertex figure of



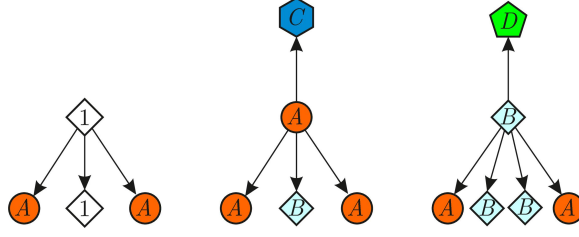


Figure 8: Growing method in case of the faces

$C$  or  $D$  a vertex  $W_{i-1}$  can be vertex  $A$  or  $B$ , respectively. In the figures we denote vertices type  $C$  by blue hexagons, vertices type  $D$  by green pentagons and vertices type  $E$  by yellow squares. The blue thick directed edges are mosaic-edges between levels  $i-1$  and  $i$ , while the red thin ones are between levels  $i$  and  $i+1$ . We mention that in case of Pascal's pyramid there are only type  $C$  inner vertices.

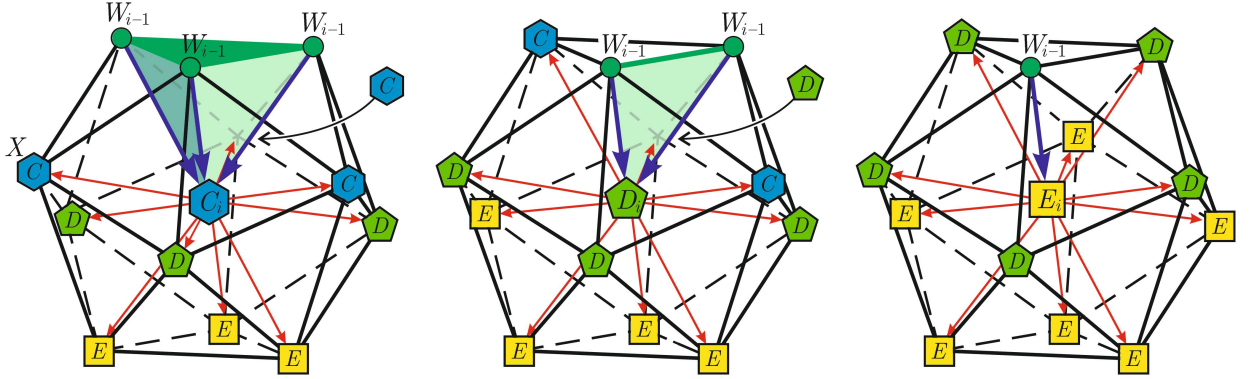


Figure 9: Growing method in case of the inner vertices with icosahedra

In Figure 10 the growing method is presented in case of the inner vertices. They come from the centres and vertices from the icosahedra in Figure 9.

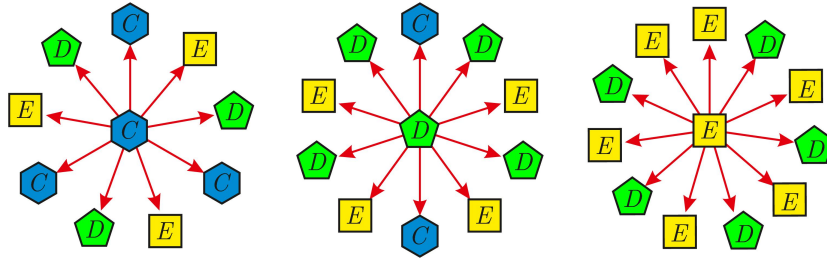


Figure 10: Growing method in case of the inner vertices

Three new  $C$ ,  $D$  and  $E$  connect for all vertices type  $C$ , but from the explanation above all new vertices  $C$  and  $D$  connect altogether three or two other vertices on level  $i$ , respectively. So, for the correct calculation we correspond just one third or half of them to the examined vertices  $C$ , respectively. All the new vertices  $C$  connect to just one vertex on level  $i$ . By the

help of the similar consideration in case of vertices  $D$  and  $E$ , we can calculate the number of vertices on level  $i + 1$ , recursively, without multiplicity.

Finally, we denote the sums of vertices types  $A$ ,  $B$ ,  $C$ ,  $D$  and  $E$  on level  $i$  by  $a_i$ ,  $b_i$ ,  $c_i$ ,  $d_i$  and  $e_i$ , respectively.

Summarising the details ( $i \geq 4$ ) and calculating the numbers of vertices in some lower levels ( $i < 4$ ) from Table 1, we prove the Theorem 1.

**Theorem 1.** *The growing of the numbers of the different types of the vertices are described by the system of linear inhomogeneous recurrence sequences ( $n \geq 1$ )*

$$\begin{aligned}
 a_{n+1} &= a_n + b_n + 3, \\
 b_{n+1} &= a_n + 2b_n, \\
 c_{n+1} &= \frac{1}{3}a_n + c_n + \frac{2}{3}d_n, \\
 d_{n+1} &= \frac{1}{2}b_n + \frac{3}{2}c_n + 2d_n + \frac{5}{2}e_n, \\
 e_{n+1} &= 3c_n + 4d_n + 6e_n,
 \end{aligned} \tag{1}$$

with zero initial values.

Moreover, let  $s_n$  be the number of all the vertices on level  $n$ , so that  $s_0 = 1$  and

$$s_n = a_n + b_n + c_n + d_n + e_n + 3 \quad (n \geq 1).$$

Table 1 shows the numbers of the vertices on levels up to 10.

$n$	0	1	2	3	4	5	6	7	8	9	10
$a_n$	0	0	3	6	12	27	66	168	435	1134	2964
$b_n$	0	0	0	3	12	36	99	264	696	1827	4788
$c_n$	0	0	0	1	3	9	34	174	1128	8251	63315
$d_n$	0	0	0	0	3	24	177	1347	10467	82029	644808
$e_n$	0	0	0	0	3	39	357	2952	23622	186984	1474773
$s_n$	1	3	6	13	36	138	736	4908	36351	280228	2190651

Table 1: *Number of types of vertices ( $n \leq 10$ )*

**Theorem 2.** *The sequences  $\{a_n\}$ ,  $\{b_n\}$ ,  $\{c_n\}$ ,  $\{d_n\}$ ,  $\{e_n\}$  and  $\{s_n\}$  can be described by the same fifth order linear homogeneous recurrence sequence*

$$x_n = 12x_{n-1} - 37x_{n-2} + 37x_{n-3} - 12x_{n-4} + x_{n-5} \quad (n \geq 6), \tag{2}$$

the initial values are in Table 1. The sequences  $\{a_n\}$ ,  $\{b_n\}$  can be also described by

$$x_n = 4x_{n-1} - 4x_{n-2} + x_{n-3} \quad (n \geq 4). \tag{3}$$



Moreover, the explicit formulae

$$\begin{aligned}
a_n &= \left(-\frac{9}{2} + \frac{21}{10}\sqrt{5}\right) \alpha_1^n + \left(-\frac{9}{2} - \frac{21}{10}\sqrt{5}\right) \alpha_2^n + 3, \\
b_n &= \left(3 - \frac{6}{5}\sqrt{5}\right) \alpha_1^n + \left(3 + \frac{6}{5}\sqrt{5}\right) \alpha_2^n - 3, \\
c_n &= \left(-\frac{33}{10} + \frac{3}{2}\sqrt{5}\right) \alpha_1^n + \left(-\frac{33}{10} - \frac{3}{2}\sqrt{5}\right) \alpha_2^n + \left(\frac{122}{15} - \frac{21}{10}\sqrt{15}\right) \alpha_3^n \\
&\quad + \left(\frac{122}{15} + \frac{21}{10}\sqrt{15}\right) \alpha_4^n + \frac{1}{3}, \\
d_n &= \left(\frac{27}{5} - \frac{12}{5}\sqrt{5}\right) \alpha_1^n + \left(\frac{27}{5} + \frac{12}{5}\sqrt{5}\right) \alpha_2^n + \left(-\frac{213}{20} + \frac{11}{4}\sqrt{15}\right) \alpha_3^n \\
&\quad + \left(-\frac{213}{20} - \frac{11}{4}\sqrt{15}\right) \alpha_4^n - \frac{3}{2}, \\
e_n &= \left(-\frac{21}{10} + \frac{9}{10}\sqrt{5}\right) \alpha_1^n + \left(-\frac{21}{10} - \frac{9}{10}\sqrt{5}\right) \alpha_2^n + \left(\frac{31}{10} - \frac{4}{5}\sqrt{15}\right) \alpha_3^n \\
&\quad + \left(\frac{31}{10} + \frac{4}{5}\sqrt{15}\right) \alpha_4^n + 1, \\
s_n &= \left(-\frac{3}{2} + \frac{9}{10}\sqrt{5}\right) \alpha_1^n + \left(-\frac{3}{2} - \frac{9}{10}\sqrt{5}\right) \alpha_2^n + \left(\frac{7}{12} - \frac{3}{20}\sqrt{15}\right) \alpha_3^n \\
&\quad + \left(\frac{7}{12} + \frac{3}{20}\sqrt{15}\right) \alpha_4^n + \frac{17}{6}
\end{aligned}$$

are valid, where  $\alpha_1 = (3 + \sqrt{5})/2$ ,  $\alpha_2 = (3 - \sqrt{5})/2$ ,  $\alpha_3 = 4 + \sqrt{15}$  and  $\alpha_4 = 4 - \sqrt{15}$ .

For the proof of Theorem 2 we apply Theorem 3.

**Theorem 3.** Let the real linear homogeneous recurrence sequences  $a^{(j)}$  embedded in each other be given the following way ( $k \geq 2$ ,  $i \geq 0$ ,  $j = 1, 2, \dots, k$ )

$$\begin{aligned}
a_{i+1}^{(1)} &= m_{1,1}a_i^{(1)} + m_{1,2}a_i^{(2)} + \dots + m_{1,k}a_i^{(k)} \\
a_{i+1}^{(2)} &= m_{2,1}a_i^{(1)} + m_{2,2}a_i^{(2)} + \dots + m_{2,k}a_i^{(k)} \\
&\vdots \\
a_{i+1}^{(k)} &= m_{k,1}a_i^{(1)} + m_{k,2}a_i^{(2)} + \dots + m_{k,k}a_i^{(k)},
\end{aligned}$$

with initial values  $a_0^{(j)} \in \mathbb{R}$  and

$$r_{i+1} = \alpha_1 a_i^{(1)} + \alpha_2 a_i^{(2)} + \dots + \alpha_k a_i^{(k)}, \quad r_0 \in \mathbb{R}.$$

In a shorter form

$$\mathbf{a}_{i+1} = \mathbf{M}\mathbf{a}_i, \tag{4}$$

$$r_{i+1} = \boldsymbol{\alpha}^T \mathbf{a}_i, \tag{5}$$

where  $\mathbf{M} = \{m_{i,j}\}_{k \times k}$ ,  $\mathbf{a}_j = [a_j^{(1)} \ a_j^{(2)} \ \dots \ a_j^{(k)}]^T$ ,  $\boldsymbol{\alpha} = [\alpha_1 \ \alpha_2 \ \dots \ \alpha_k]^T$  and  $\text{rank}(\mathbf{M}) = k$ . If  $\beta_i \in \mathbb{R}$  and

$$r_i = \beta_1 r_{i-1} + \beta_2 r_{i-2} + \dots + \beta_k r_{i-k}, \quad (i \geq k) \quad (6)$$

then  $\beta_i$  are the coefficients of characteristic polynomial of matrix  $\mathbf{M}$ .

Moreover, if the matrix  $\mathbf{M}$  has  $\ell$  distinct eigenvalues with one algebraic multiplicity and  $\gamma_j$  ( $1 \leq j \leq \ell$ ) are the coefficients of minimal polynomial of  $\mathbf{M}$ , then

$$r_i = \gamma_1 r_{i-1} + \gamma_2 r_{i-2} + \dots + \gamma_\ell r_{i-\ell} \quad (i \geq k \geq \ell). \quad (7)$$

*Proof.* From (4) and (5) we obtain, that

$$\begin{aligned} r_i = \boldsymbol{\alpha}^T \mathbf{a}_{i-1} &= \boldsymbol{\alpha}^T \mathbf{M} \mathbf{a}_{i-2} = \boldsymbol{\alpha}^T \mathbf{M}^2 \mathbf{a}_{i-3} = \dots = \boldsymbol{\alpha}^T \mathbf{M}^{k-1} \mathbf{a}_{i-k}, \\ r_{i-j} &= \boldsymbol{\alpha}^T \mathbf{M}^{k-(j+1)} \mathbf{a}_{i-k} \quad (j = 0, 1, \dots, k-1). \end{aligned}$$

It follows from  $\text{rank}(\mathbf{M}) = k$  (has inverse), that

$$r_{i-k} = \boldsymbol{\alpha}^T \mathbf{M}^{-1} \mathbf{a}_{i-k}.$$

We substitute the results into (6),

$$\begin{aligned} \boldsymbol{\alpha}^T \mathbf{M}^{k-1} \mathbf{a}_{i-k} &= \beta_1 \boldsymbol{\alpha}^T \mathbf{M}^{k-2} \mathbf{a}_{i-k} + \dots + \beta_j \boldsymbol{\alpha}^T \mathbf{M}^{k-(j+1)} \mathbf{a}_{i-k} + \dots + \beta_k \boldsymbol{\alpha}^T \mathbf{M}^{-1} \mathbf{a}_{i-k} \\ &= \sum_{j=1}^k \left( \beta_j \boldsymbol{\alpha}^T \mathbf{M}^{k-(j+1)} \mathbf{a}_{i-k} \right) = \boldsymbol{\alpha}^T \left( \sum_{j=1}^k \left( \beta_j \mathbf{M}^{k-(j+1)} \right) \right) \mathbf{a}_{i-k}. \end{aligned}$$

We gain, that

$$\boldsymbol{\alpha}^T \left( \mathbf{M}^{k-1} - \sum_{j=1}^k \left( \beta_j \mathbf{M}^{k-(j+1)} \right) \right) \mathbf{a}_{i-k} = 0.$$

As  $\boldsymbol{\alpha}^T$  and  $\mathbf{a}_{i-k}$  can be any elements of the vector space  $\mathbb{R}^k$ ,

$$\mathbf{M}^{k-1} - \sum_{j=1}^k \left( \beta_j \mathbf{M}^{k-(j+1)} \right) = \mathbf{0},$$

thus

$$\mathbf{M}^k = \sum_{j=1}^k \beta_j \mathbf{M}^{k-j}. \quad (8)$$

Using the well-known *Cayley-Hamilton Theorem*, from (8) the equation

$$x^k = \beta_1 x^{k-1} + \beta_2 x^{k-2} + \dots + \beta_k$$

is the characteristic equation of matrix  $\mathbf{M}$ . If the matrix  $\mathbf{M}$  has  $\ell$  distinct eigenvalues with one algebraic multiplicity and  $\gamma_j$  are the coefficients of the minimal polynomial of  $\mathbf{M}$ , then the method of the proof can be followed step by step for  $\ell$  elements of  $r_i$  and for  $\gamma_j$  coefficients too, thus (7) also holds. ■

*Proof of Theorem 2.* Let  $v_n = 3$  ( $n \geq 1$ ) be a constant sequence and  $v_0 = 1$ . The value  $v_n$  gives the number of vertices type “1” on level  $n$ . Substitute  $3 = v_n$  into the first equation of (1) and complete the equations system (1) with  $v_{n+1} = v_n$ . Than we have the system of linear homogeneous recurrence sequences ( $n \geq 1$ )

$$\begin{aligned} a_{n+1} &= a_n + b_n + v_n, \\ b_{n+1} &= a_n + 2b_n, \\ c_{n+1} &= \frac{1}{3}a_n + c_n + \frac{2}{3}d_n, \\ d_{n+1} &= \frac{1}{2}b_n + \frac{3}{2}c_n + 2d_n + \frac{5}{2}e_n, \\ e_{n+1} &= 3c_n + 4d_n + 6e_n, \\ v_{n+1} &= v_n \end{aligned}$$

and

$$s_n = a_n + b_n + c_n + d_n + e_n + v_n \quad (n \geq 0).$$

Using the results of Theorem 3 when

$$\mathbf{M} = \begin{pmatrix} 1 & 1 & 0 & 0 & 0 & 1 \\ 1 & 2 & 0 & 0 & 0 & 0 \\ \frac{1}{3} & 0 & 1 & \frac{2}{3} & 0 & 0 \\ 0 & \frac{1}{2} & \frac{3}{2} & 2 & \frac{5}{2} & 0 \\ 0 & 0 & 3 & 4 & 6 & 0 \\ 0 & 0 & 0 & 0 & 0 & 1 \end{pmatrix},$$

$\mathbf{a}_j = [a_j \ b_j \ c_j \ d_j \ e_j \ v_j]^T$ , and  $\text{rank}(\mathbf{M}) = 6$  we gain that the solutions of system of linear recurrence equations (8) are  $\beta_1 = 12 - t$ ,  $\beta_2 = -37 + 12t$ ,  $\beta_3 = 37 - 37t$ ,  $\beta_4 = -12 + 37t$ ,  $\beta_5 = 1 - 12t$ ,  $\beta_6 = t$ , where  $t \in \mathbb{R}$ . As  $r_n$  was an arbitrary equation,  $r_n$  can be  $s_n$ ,  $a_n$ ,  $\dots$   $e_n$  with  $\boldsymbol{\alpha} = (1, 1, 1, 1, 1, 1)$ ,  $\boldsymbol{\alpha} = (1, 0, 0, 0, 0, 0)$ ,  $\dots$ ,  $\boldsymbol{\alpha} = (0, 0, 0, 0, 1, 0)$ , respectively. Moreover, let  $t = 0$ , then we obtain the (degenerate) recurrence sequence (2).

As  $a_{n+1}$ ,  $b_{n+1}$  and  $v_{n+1}$  are independent from  $c_n$ ,  $d_n$  and  $e_n$ , they form a system of homogeneous recurrence equations again with matrix  $\mathbf{M}_{ab} = \begin{pmatrix} 1 & 1 & 1 \\ 1 & 2 & 0 \\ 0 & 0 & 1 \end{pmatrix}$ . Using the results of Theorem 3 again we gain  $\beta_1 = 4$ ,  $\beta_2 = -4$ ,  $\beta_3 = 1$ , so the equation (3) holds.

The characteristic equation of (2) is

$$x^5 = 12x^4 - 37x^3 + 37x^2 - 12x + 1 \quad (9)$$

and its solutions are  $\alpha_1 = (3 + \sqrt{5})/2$ ,  $\alpha_2 = (3 - \sqrt{5})/2$ ,  $\alpha_3 = 4 + \sqrt{15}$  and  $\alpha_4 = 4 - \sqrt{15}$  and  $\alpha_5 = 1$ . We mention that equation (9) is the minimal polynomial of the matrix  $\mathbf{M}$ . (The roots of the characteristic equation of (3),  $x^3 = 4x^2 - 4x + 1$  are also  $\alpha_1$ ,  $\alpha_2$  and  $\alpha_5$ .) A suitable linear combination of their  $n^{\text{th}}$  power provide the explicit formulae ([8]). ■

**Remark 1.** In Pascal's pyramid the equations system (1) also holds with suitable initial values. In this case, there is no type vertices  $B$ ,  $D$  and  $E$ , so  $b_i = d_i = e_i = 0$  for any  $i$ . Thus the hyperbolic Pascal pyramid is not only the geometric but also the algebraic generalization of Pascal's pyramid.

**Remark 2.** *The ratios of numbers of vertices from level to level tend to the biggest eigenvalue of the matrix  $\mathbf{M}$ . So, the growing ratio of  $\mathcal{HP}$  is  $\alpha_3 = 4 + \sqrt{15} \approx 7.873$ , on the contrary it is 1 in case of the Euclidean case.*

## 4 Sum of the values on levels in the hyperbolic Pascal pyramid

The sum of the values of the elements on level  $n$  in the classical Pascal's pyramid is  $3^n$  ([4]). In this section we determine it in case of the hyperbolic Pascal pyramid.

Denote respectively  $\hat{a}_n, \hat{b}_n, \hat{c}_n, \hat{d}_n$  and  $\hat{e}_n$  the sums of the values of vertices type  $A, B, C, D$  and  $E$  on level  $n$ , and let  $\hat{s}_n$  be the sum of all the values. From Figures 8 and 10 the results of Theorem 4 can be read directly. For example for all vertices type  $A, B$  and 1 on level  $i$  generate two vertices type  $A$  on level  $i + 1$  and it follows the first equation of (10). Table 2 shows the sum of the values of the vertices on levels up to 10.

**Theorem 4.** *If  $n \geq 1$ , then*

$$\begin{aligned} \hat{a}_{n+1} &= 2\hat{a}_n + 2\hat{b}_n + 6, \\ \hat{b}_{n+1} &= \hat{a}_n + 2\hat{b}_n, \\ \hat{c}_{n+1} &= \hat{a}_n + 3\hat{c}_n + 2\hat{d}_n, \\ \hat{d}_{n+1} &= \hat{b}_n + 3\hat{c}_n + 4\hat{d}_n + 5\hat{e}_n, \\ \hat{e}_{n+1} &= 3\hat{c}_n + 4\hat{d}_n + 6\hat{e}_n \end{aligned} \tag{10}$$

*with zero initial values.*

Table 2 shows the sums of values on levels up to 10.

$n$	0	1	2	3	4	5	6	7	8	9	10
$a_n$	0	0	6	18	54	174	582	1974	6726	22950	78342
$b_n$	0	0	0	6	30	114	402	1386	4746	16218	55386
$c_n$	0	0	0	6	36	210	1452	12138	114684	1147002	11729148
$d_n$	0	0	0	0	24	324	3600	38148	398112	4132596	42818208
$e_n$	0	0	0	0	18	312	3798	41544	438270	4566120	47368110
$s_n$	1	3	9	33	165	1137	9837	95193	962541	9884889	102049197

Table 2: *Sum of values of vertices ( $n \leq 10$ )*

Let  $\hat{s}_n$  be the sum of the values of all the vertices on level  $n$ , then  $\hat{s}_0 = 1$  and

$$\hat{s}_n = \hat{a}_n + \hat{b}_n + \hat{c}_n + \hat{d}_n + \hat{e}_n + 3 \quad (n \geq 1).$$

**Theorem 5.** *The sequences  $\{\hat{a}_n\}$ ,  $\{\hat{b}_n\}$ ,  $\{\hat{c}_n\}$ ,  $\{\hat{d}_n\}$ ,  $\{\hat{e}_n\}$  and  $\{\hat{s}_n\}$  can be described by the same sixth order linear homogeneous recurrence sequence*

$$\hat{x}_n = 18\hat{x}_{n-1} - 99\hat{x}_{n-2} + 226\hat{x}_{n-3} - 224\hat{x}_{n-4} + 92\hat{x}_{n-5} - 12\hat{x}_{n-6} \quad (n \geq 7),$$

*the initial values are in Table 2. The sequences  $\{\hat{a}_n\}$ ,  $\{\hat{b}_n\}$  can be also described by*

$$\hat{x}_n = 5\hat{x}_{n-1} - 6\hat{x}_{n-2} + 2\hat{x}_{n-3} \quad (n \geq 4).$$

*The explicit formulae*

$$\begin{aligned} \hat{a}_n &= \left(\frac{9}{2}\sqrt{2} - 6\right) (2 + \sqrt{2})^n + \left(\frac{9}{2}\sqrt{2} - 6\right) (2 - \sqrt{2})^n + 6, \\ \hat{b}_n &= \left(\frac{9}{2} - 3\sqrt{2}\right) (2 + \sqrt{2})^n + \left(\frac{9}{2} + 3\sqrt{2}\right) (2 - \sqrt{2})^n - 6 \end{aligned}$$

*and*

$$\hat{s}_n = 3 + \frac{3}{2}(\sqrt{2} - 1)(2 + \sqrt{2})^n - \frac{3}{2}(\sqrt{2} + 1)(2 - \sqrt{2})^n + \delta_4\alpha_4 + \delta_5\alpha_5 + \delta_6\alpha_6,$$

*where if  $\varphi = \arctan(9\sqrt{101}/128)/3$ , then  $\alpha_4 = (-\sqrt{85}\cos(\varphi) - \sqrt{3}\sqrt{85}\sin(\varphi) + 13)/3 \approx 0.240683$ ,  $\alpha_5 = (-\sqrt{85}\cos(\varphi) + \sqrt{3}\sqrt{85}\sin(\varphi) + 13)/3 \approx 2.408387$  and  $\alpha_6 = (2\sqrt{85}\cos(\varphi) + 13)/3 \approx 10.350930$  are the roots of the equation  $x^3 - 13x^2 + 28x - 6 = 0$ , moreover  $\delta_4 \approx 1.137480$ ,  $\delta_5 \approx -0.144699$  and  $\delta_6 \approx 0.007219$ .*

*Proof.* Follow the proof of Theorem 2 step by step. Using the results of Theorem 4 when

$$\mathbf{M} = \begin{pmatrix} 2 & 2 & 0 & 0 & 0 & 2 \\ 1 & 2 & 0 & 0 & 0 & 0 \\ 1 & 0 & 3 & 2 & 0 & 0 \\ 0 & 1 & 3 & 4 & 5 & 0 \\ 0 & 0 & 3 & 4 & 6 & 0 \\ 0 & 0 & 0 & 0 & 0 & 1 \end{pmatrix}, \quad \mathbf{M}_{ab} = \begin{pmatrix} 2 & 2 & 2 \\ 1 & 2 & 0 \\ 0 & 0 & 1 \end{pmatrix},$$

we gain that  $\beta_1 = 18$ ,  $\beta_2 = -99$ ,  $\beta_3 = 226$ ,  $\beta_4 = -224$ ,  $\beta_5 = 92$ ,  $\beta_6 = -12$  and the characteristic polynomial of  $\mathbf{M}$  is  $(x - 1)(x^2 - 4x + 2)(x^3 - 13x^2 + 28x - 6)$  and its roots are  $\alpha_i$  ( $i = 1, \dots, 6$ ). As the exact values of coefficients  $\delta_j$  ( $j = 4, 5, 6$ ) are very complicated (for sequences  $\hat{c}_n$ ,  $\hat{d}_n$ ,  $\hat{e}_n$  also), we give their numerical values in case sequence  $\hat{s}_n$  by the help of MAPLE software. But from the characteristics polynomial of  $\mathbf{M}_{ab}$  the sequences  $\hat{a}_n$  and  $\hat{b}_n$  are given in exact explicit forms. ■

**Remark 3.** *The growing ratio of values of  $\mathcal{HPP}$  is  $\approx 10.351$ , while it is 3 in case of the Euclidean case.*

## References

- [1] Ahmia, M. – Szalay, L., On the weighted sums associated to rays in generalized Pascal triangle, submitted.
- [2] Belbachir, H., Németh, L., Szalay, L., Hyperbolic Pascal triangles, Applied Mathematics and Computation, to appear (arXiv:1503.02569).
- [3] Belbachir, H. – Szalay, L., On the arithmetic triangles, Šiauliai Math. Sem., **9** (17) (2014), 15-26.
- [4] Bondarenko, B. A., Generalized Pascal triangles and pyramids, their fractals, graphs, and applications. Translated from the Russian by Bollinger, R. C. (English) Santa Clara, CA: The Fibonacci Association, vii, 253 p. (1993). [www.fq.math.ca/pascal.html](http://www.fq.math.ca/pascal.html)
- [5] Coxeter, H. S. M., Regular honeycombs in hyperbolic space, Proc. Int. Congress Math., Amsterdam, Vol. III. (1954), 155-169.
- [6] Harris, J. M., Hirst, J. L., Mossinghoff, M. J., Combinatorics and Graph Theory, Springer, (2008).
- [7] Németh, L., Szalay, L., Alternating sums in hyperbolic Pascal triangles, submitted.
- [8] Shorey, T. N., – Tijdeman, R., Exponential diophantine equation, Cambridge University Press, 1986, p. 33.